I&EC research
Industrial & Engineering Chemistry Research

Article

pubs.acs.org/IECR

Preparation and Performance of Polyimide-Reinforced Clay Aerogel Composites

Wei Wu, Kai Wang,* and Mao-Sheng Zhan

Key Laboratory of Aerospace Materials and Service of Ministry of Education, School of Materials Science and Engineering, Beihang University, Beijing 100191, P.R. China

ABSTRACT: Low-density polyimide (PI)/clay aerogel composites were produced by freeze-drying of a poly(amic acid) ammonium salt/clay precursor suspension, followed by a multistep temperature-programmed imidization. The densities of the resulting aerogel composites were in the range of 0.04−0.09 g·cm^{-3}. With the increase of PI content, a more perfect "layer−strut" bracing structure was exhibited in the composites, which resulted in vastly improved mechanical properties. Polyimide did not intercalate the interlayer of clay, and the onset decomposition temperatures (T_d) of the aerogels were more than 410 °C. The obtained PI/clay aerogel composites show considerable promise in structural and high-temperature insulation applications.

1. INTRODUCTION

Aerogels are porous solid materials consisting of more than 90% air in the form of interconnected three-dimensional network structure. Because of the nanoporous structure, aerogels exhibit many unique properties, including ultralow density, large surface area, low thermal conductivity, and high acoustic attenuation. Thus, aerogels are promising materials for various applications, such as thermal insulation, acoustic insulation, catalysis, adsorption, sensing, and drug delivery.

Early in 1953, Hofmann successfully prepared the first clay aerogel by freeze-drying clay hydrogel.[1] Call also described this method in detail later that year.[2] After that, several other researchers studied the effect of process condition and composition on the structure.[3−6] Unfortunately, neat clay aerogels are so weak that they are easily damaged under low-stress conditions. As the earliest aerogel material, silica aerogel was limited by its extreme fragility. Some researchers, such as Leventis and co-workers,[7−11] reported an enhancement method involving increasing the strength of the interparticle necks between secondary particles in silica aerogel by introducing cross-linkable isocyanate or epoxy precursors, which effectively broadened their application potential. Recently, several research works on modified clay aerogel materials were reported by the Schiraldi group,[12−22] and clay aerogels have begun to receive considerable attention from researchers once again. Investigators have introduced water-soluble polymers or fibers into clay aerogels that effectively improve the compressive strength and modulus of the aerogels. Several kinds of organic polymers have been used, such as poly(*N*-isopropylacrylamide),[12] thermoset epoxy,[13] casein,[14,15] poly(vinyl alcohol),[16−18] poly(ethylene imine),[19] and poly(acrylic acid).[20] A similar enhancement effect was also achieved by adding natural or synthetic fiber.[21,22] Some typical structures were formed in these aerogel composites, for example, interpenetrating cocontinuous network structures,[14,15] random dendritic-type structures,[16] "warp−weft" woven-like structures,[21] and "wattle and daub" structures.[22] Nevertheless, most of the reinforcements have had poor thermal stabilities, which greatly constrains the utilization of these aerogel composites.

Because of the rigid aromatic structure of the imide chain, polyimides have good mechanical properties, excellent thermal stability, and high glass transition temperatures, and they are used as high-performance polymers in many fields.[23,24] Actually, polyimide aerogels, which are usually prepared from polyimide gels by a supercritical CO_2 drying process, have also been reported in the past few years.[25−29] PI aerogels not only have the typical characteristics of ordinarily organic aerogels but also show good heat resistance. As a result, polyimide could be used to strengthen clay aerogels while retaining the good thermal stability of these materials. However, almost all polyimides cannot be dissolved in water, which restricts the direct introduction of polyimide into clay aerogel. In this work, poly(amic acid) ammonium salt was used as a water-soluble precursor to blend with clay in water, followed by freeze-drying and thermal imidization to produce PI/clay aerogel composites.

2. EXPERIMENTAL SECTION

2.1. Materials. 4,4′-Oxydianiline (ODA, 98%) was purchased from Sinopharm Chemical Reagent Co. and used as received. Pyromellitic dianhydride (PMDA, 99%) was supplied by Liyang Qingfeng Fine Chemical Co. and dried in a vacuum oven at 180 °C for 6 h prior to use. *N*,*N*-Dimethylacetamide (DMAc, 99.5%) and triethylamine (TEA, 99%) were both provided by Beijing Chemical Works, and 3-aminopropyltrimethoxysilane (APTMOS, 95%) was obtained from Acros Co.; these chemicals were all used without further modification. Sodium montmorillonite [Na^+-MMT, PGW grade, cation-exchange capacity (CEC), 90 mequiv/100 g) was purchased from Zhejiang Fenghong New Material Co. Deionized water was obtained from China Agricultural University.

2.2. Preparation of Water-Soluble Polyimide Precursor Solution. 4,4′-ODA and DMAc were added into a 250 mL

Received: June 19, 2012
Revised: September 7, 2012
Accepted: September 10, 2012
Published: September 10, 2012

dx.doi.org/10.1021/ie301622s | *Ind. Eng. Chem. Res.* 2012, 51, 12821−12826

three-neck round-bottom flask fitted with a mechanical stirrer. Once the ODA had dissolved completely, a specified quantity of PMDA was added, and the mixture was stirred for 4 h; subsequently, APTMOS was slowly dropped into the mixture. Note that the PMDA/4,4′-ODA/APTMOS molar ratio was 100:99:2. An APTMOS-capped poly(amic acid) (AP-PAA) solution with a solid content of 12 wt % was obtained after continued stirring of the reaction mixture for another 4 h. Then, the resultant solution was poured into deionized water and deposited. After washing, drying, and crushing, AP-PAA powder was obtained. The ammonium salt solution of AP-PAA was prepared from AP-PAA (1 g) and TEA (0.48 g) in deionized water (18.52 g) (5 wt % AP-PAA). The solution was continuously stirred at room temperature until it became homogeneous and transparent.

2.3. Preparation of Polyimide/Clay Aerogel Composites. A series of PI/clay aerogel composites with different compositions were prepared and are denoted as C5P*x*, where "5" represents the clay concentration and *x* represents the AP-PAA content (calculated from the weight of AP-PAA relative to that of clay). For example, 3 g of the above AP-PAA salt solution (0.15 g of AP-PAA), 1.5 g of Na^+-MMT, and 27.22 g of deionized water were poured into a vessel. The mixture was blended to wet the clay by hand; then, it was mixed at high speed using a Kaiser electric mixer for four intervals of 15 s to create the C5P10 sample. Afterward, the resulting suspension was transferred to 5 mL cylindrical vials, frozen in a −45 °C ethanol bath, and dried in a Four-Ring LGJ-10A freeze-dryer. After 24−36 h in the lyophilizer, the samples were removed and heated under a vacuum for 1 h at 80, 120, 160, 200, 250, and 300 °C. (If the imidization was complete, the weight of PI in the C5P10 sample accounted for 9.14% of the clay.)

2.4. Characterization. The densities of the PI/clay aerogel composites were calculated by measuring mass and dimensions using a Sartorius BS124S electronic balance and a slide caliper, respectively. Fourier transform infrared (FTIR) spectra were recorded on a Nicolet NEXUS-470 spectrometer for PI/clay aerogel composites before and after imidization. A CS-3400 scanning electron microscopy (SEM) system was used to observe the aerogel microstructures. Compression testing was carried out using an Instron model 3365 universal testing machine, equipped with a 100-N load cell, at a constant crosshead speed of 0.8 mm/min. X-ray diffraction (XRD) patterns of aerogel composites were characterized on a D/max2200 PC automatic X-ray diffractometer. Thermogravimetric analysis (TGA) was conducted on a TA Instruments Q50 thermogravimetric analyzer at a heating rate of 10 °C/min from room temperature to 800 °C under nitrogen atmosphere.

3. RESULTS AND DISCUSSION

The overall preparation process of water-soluble polyimide precursor solution is shown in Scheme 1. First, poly(amic acid) intermediate was generated from the reaction of 4,4′-ODA and PMDA. Then, silicon-containing monoamine (APTMOS) was incorporated to form AP-PAA. Finally, poly(amic acid) salt solution was prepared by dissolving AP-PAA in an aqueous solution of TEA. Moreover, the silicon-containing group located at the end of the molecule chain can produce physical or chemistry forces with the clay mineral and improve the combination of PI with clay.

Figure 1 shows a picture of PI/clay aerogel composites before and after imidization. The aerogels transformed from white to brown in appearance. During the process of freeze-drying and thermal imidization, the aerogels exhibited shrinkage of less than 8%, measured as the difference between the diameter of the mold and the final sample. Moreover, with the incorporation of AP-PAA salt, the stability of the AP-PAA salt/clay suspension gradually decreased, as a result of the flocculation effect of the polymer. Precipitation even occurred in several minutes when the AP-PAA content exceeded 30% (w/w), so this concentration was chosen as the maximum added amount.

Scheme 1. Reaction Scheme of Water-Soluble Polyimide Precursor

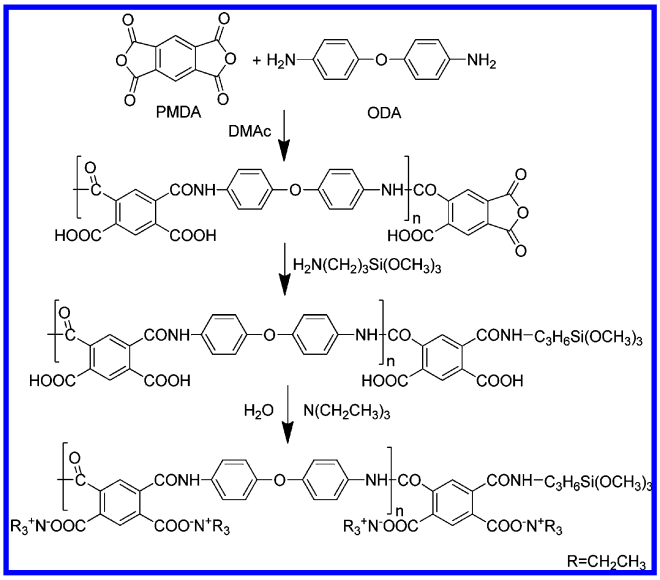

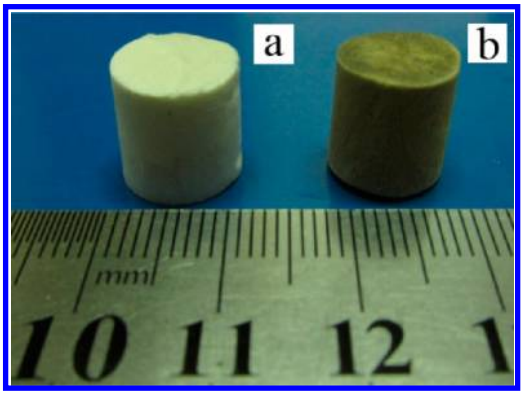

Figure 1. PI/clay aerogel composite: (a) before imidization and (b) after imidization.

The FTIR spectra of montmorillonite clay and PI/clay aerogel composites before and after imidization are presented in Figure 2. For the aerogel after imidization, the characteristic absorption peaks at 1778 and 1725 cm^{-1} are assigned to asymmetric and symmetric carbonyl (C═O) stretching vibrations of the imide ring, respectively. The absorption peak at 1380 cm^{-1} is attributed to the C−N stretching vibration of the imide ring. The presence of these characteristic peaks indicates the existence of polyimide. Furthermore, the peak at 3630 cm^{-1} is assigned to the octahedral layer hydroxyl stretching vibration,[30] and the broad bands at 3436 and 1639 cm^{-1} correspond to the hydroxyl stretching of adsorbed water molecules.[31,32] However, the hydroxyl peak is also present in the FTIR spectrum of PI/clay aerogel composite, which might be due to the absorption of atmospheric moisture. The strong

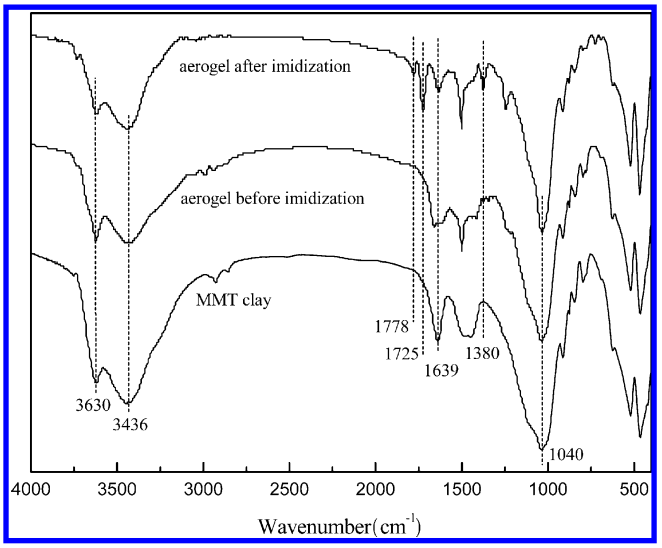

Figure 2. FTIR analysis of montmorillonite clay and PI/clay aerogel composites before and after imidization.

absorption peak at 1040 cm^{-1} is traced to the skeleton vibration of siloxane (Si−O−Si).

The morphologies of the clay aerogel and PI/clay aerogel composites were studied by SEM (see Figure 3). Because of the rearrangement effect of ice-crystal growth, all of these aerogels exhibit highly lamellar structures with a monolayer thickness of about 1 μm and a layer spacing of several tens of micrometers. Meanwhile, with increasing content of PI, the struts connecting the layers become more integral, and their overall quantity increases as well, whereas the monolayer thickness and layer spacing are barely affected. The mutual parallel layers and struts between the layers constitute a "layer−strut" bracing structure that could absorb and transfer loads effectively. This structure becomes more perfect with increased content of PI in the aerogel composites, leading to greatly improved mechanical properties.

X-ray diffraction (XRD) spectra of clay particles and the aerogels are presented in Figure 4. The clay particles show a

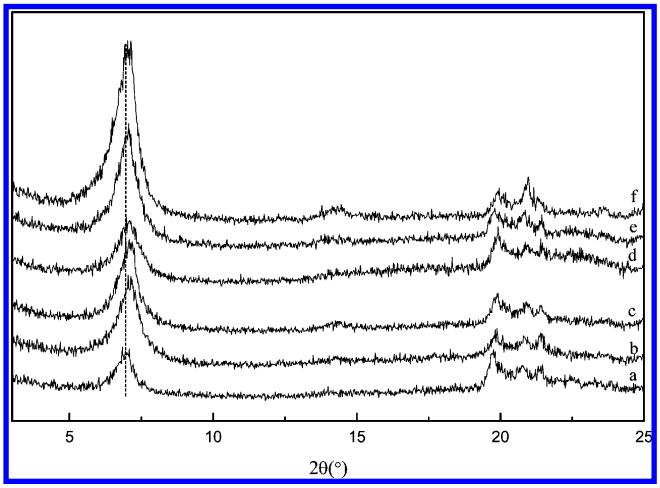

Figure 4. XRD patterns of clay particles and aerogels: (a) clay particles, (b) C5P1, (c) C5P5, (d) C5P10, (e) C5P30, and (f) C5P0.

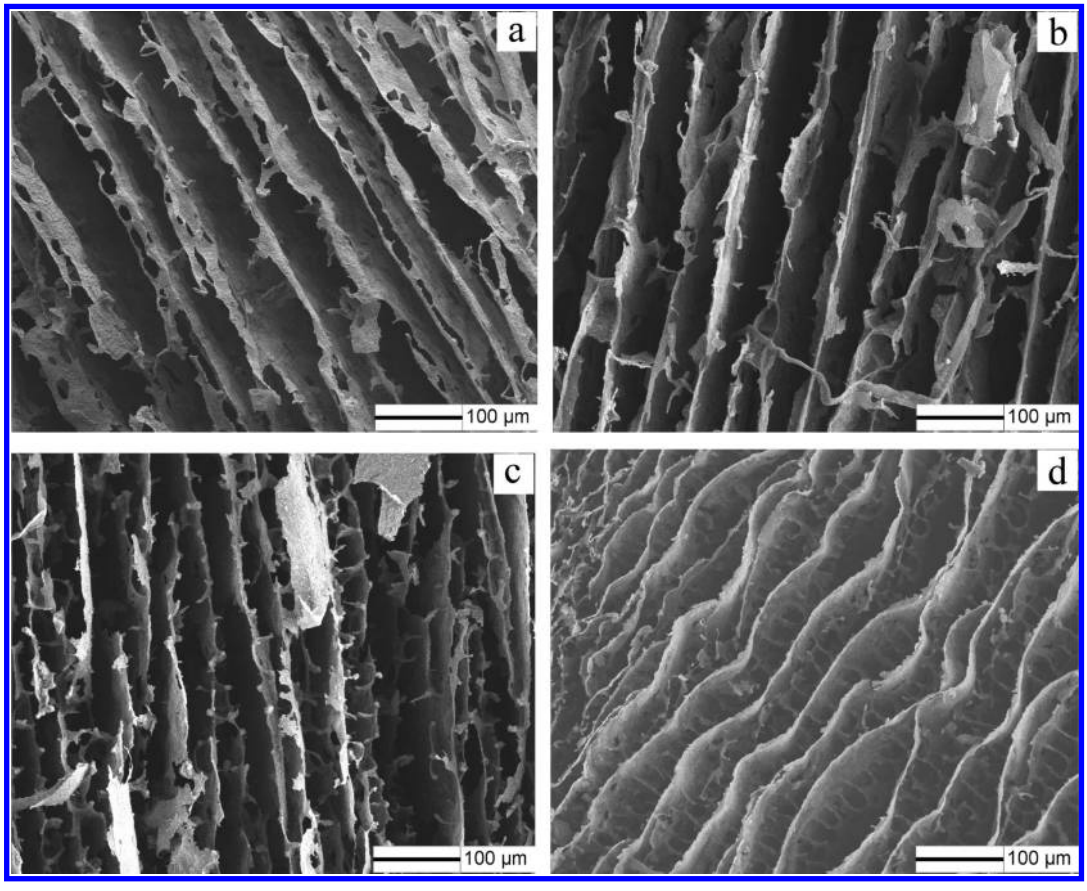

Figure 3. SEM images of aerogels with different compositions: (a) C5P0, (b) C5P1, (c) C5P10, and (d) C5P30.

dx.doi.org/10.1021/ie301622s | *Ind. Eng. Chem. Res.* 2012, 51, 12821−12826

clear diffraction peak at $2\theta = 6.95°$, whereas the characteristic peak shifts to 7.09° when clay converts to clay aerogel. According to the Bragg equation ($\lambda = 2d \sin \theta$), the interlayer spacing (d_{001} spacing) of the clay decreases from 1.27 to 1.25 nm. Simultaneously, it can be seen that the PI/clay aerogel composites have almost the same interlayer spacing as the clay aerogel. This illustrates that the polymer chains did not intercalate the clay, which is different from the behaviors of rubber[33,34] and poly(vinyl alcohol) (PVA).[17] If a polymer molecular chain inserted into the clay gallery, the conformation of the polymer would change from random coil to restricted state, which is a process of decreasing entropy. Perhaps the interaction force between the clay and AP-PAA salt chain or our experimental conditions could not provide enough energy, so the intercalation process did not occur.

As shown in Figure 5, PI/clay aerogels with different compositions were prepared. The neat clay aerogel produced

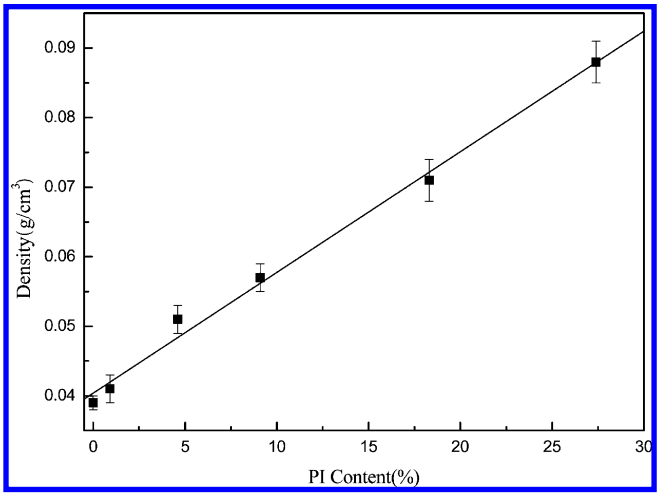

Figure 5. Aerogel density as a function of PI content.

from a 5 wt % solution in water had a density of 0.039 g·cm^{-3}. When 27.4% (w/w) PI was incorporated, the density of the aerogel sample increased to 0.088 g·cm^{-3}. A linear relationship between density and PI content was found in the range of research, suggesting that the lamellar structures of the aerogel composites are similar to each other.

The stress–strain curves and compressive modulus of the aerogel samples are displayed in Figures 6 and 7, respectively. It can be seen that the stress–strain behavior of PI/clay aerogel composites is similar to that of classical polymer foams: a linear elastic region at low strain, followed by a plateau of plastic yielding and finally a densification region where the pore space is squeezed out.[35] Because clay comprised a major constituent of the aerogel composites, the composites recovered only a negligible amount after the compression tests. In general, the compressive moduli of the samples increased linearly with increasing density. The unmodified clay aerogel had a compressive modulus of only ~7 kPa at a density of 0.039 g·cm^{-3}. After addition of 18.3% (w/w) PI, the density of the PI/clay aerogel rose to 0.071 g·cm^{-3}, and the compressive modulus sharply increased to 200.7 kPa, which is equivalent to the enhancement effect observed with PVA.[17,18] Judging from the chemical structure, PVA can interact with clay through a strong combination of hydrogen and covalent bonding,[36] and the interaction force between PI and clay is inferior to that of PVA and clay. Additionally, as shown in the XRD spectra, the

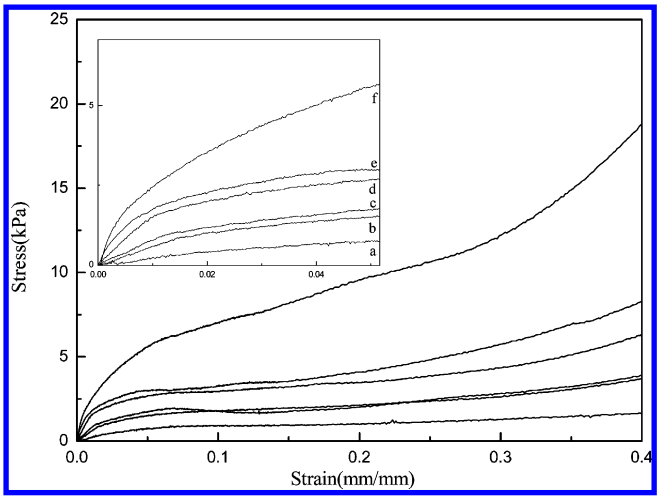

Figure 6. Compressive stress–strain curves of aerogel samples: (a) C5P0, (b) C5P1, (c) C5P5, (d) C5P10, (e) C5P20, and (f) C5P30.

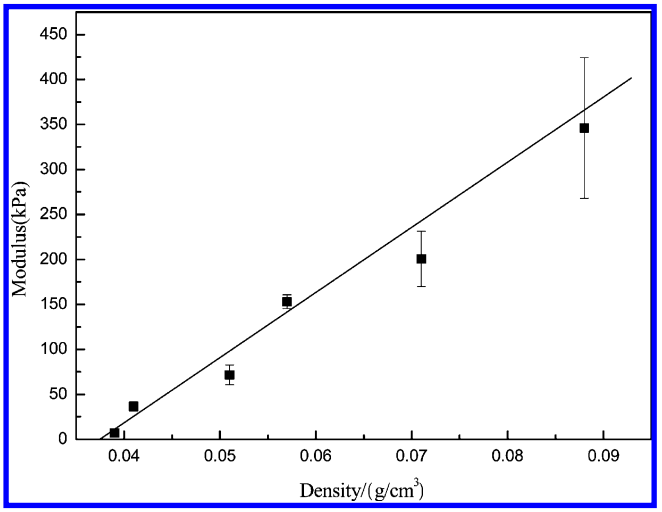

Figure 7. Compressive moduli of aerogel samples.

polyimide chain does not intercalate into the clay gallery, whereas the PVA chain could intercalate or even exfoliate the clay, giving the observed enhancement of the aerogel's mechanical properties.[17] Hence, the compressive property of PI/clay aerogel only matches that of PVA/clay aerogel. As shown in Figure 3, after the incorporation of polyimide into the clay aerogel, the structures of the aerogel composites change from "separate layer" to layer–strut, so the aerogel composites exhibit a much higher compressive modulus than the neat clay aerogel.

The thermal properties of clay powder, PI (thermal imidization from AP-PAA salt), and PI/clay aerogel composites (only C5P10 and C5P30) were evaluated by TGA (Figure 8) and differential thermogravimetry (DTG) (Figure 9). The onset decomposition temperatures (T_d), 5% weight loss temperatures ($T_{5\%}$), maximum decomposition rate temperatures (T_{max}), and residual weight retentions (R_w) at 800 °C of these materials are presented in Table 1.

It can be observed that the T_d values of C5P10 and C5P30 are 436 and 414 °C, respectively. However, they are much lower than the T_d value of clay or PI. There are two possible reasons for this phenomenon: One is that the imidization of PI in the aerogel composite was not complete. The other is that,

dx.doi.org/10.1021/ie301622s | Ind. Eng. Chem. Res. 2012, 51, 12821–12826

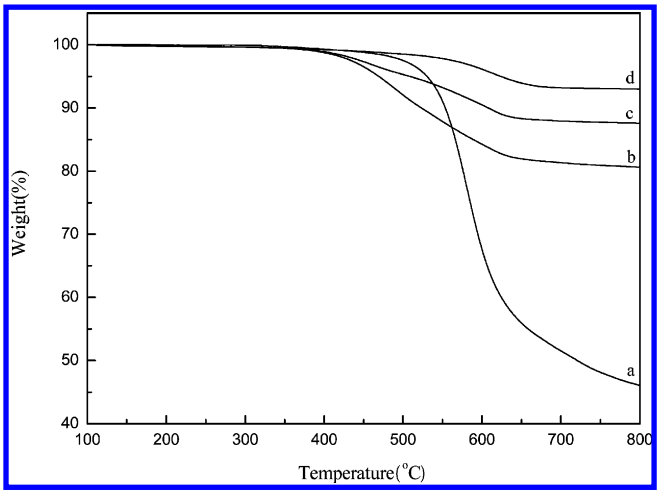

Figure 8. TGA curves of (a) PI, (b) C5P30, (c) C5P10, and (d) clay powder.

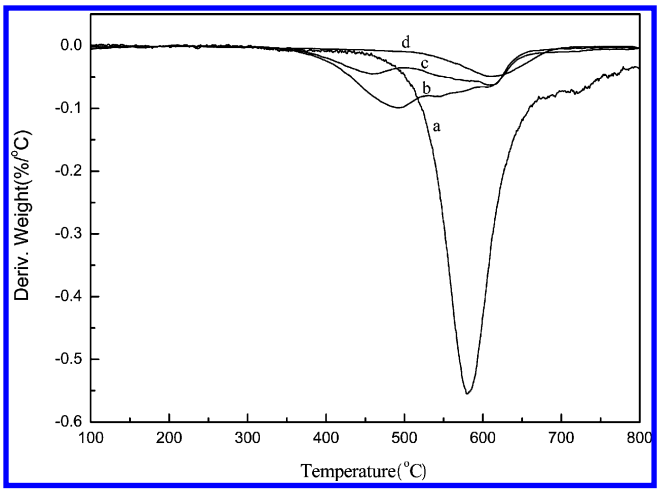

Figure 9. DTG curves of (a) PI, (b) C5P30, (c) C5P10, and (d) clay powder.

Table 1. Thermal Properties of PI/Clay Aerogel Composites

				R_w (%)	
sample	T_d (°C)	$T_{5\%}$ (°C)	T_{max} (°C)	theor	expt
clay	511	623	610	–	93.0
PI	520	531	580	–	46.1
C5P10	436	508	608	88.4	87.6
C5P30	414	469	493	81.4	80.6

although thermal imidization was complete, a few of residual TEA molecules were embedded in the clay sheets and were not released until the TGA test. The second reason is much more likely, because no characteristic absorptions of AP-PAA salt were found in the FTIR spectrum of aerogel composite after imidization and no obvious mass changes were detected in the TGA analysis of PI before 400 °C, which suggests that the AP-PAA salt can be imidized completely under the thermal process. Nonetheless, the aerogel composites have much better thermal stability than other polymer/clay aerogels, which seriously decomposed at 200–300 °C.[13−15] According to the R_w vaules of pure clay and PI, the theoretical R_w values of the PI/clay aerogel composites were calculated, as shown in Table 1. On one hand, the clay sheets could prevent the accumulated heat from being lost rapidly, which would accelerate PI decomposition. On the other hand, residual TEA was released during the TGA test. Therefore, the actual R_w values of the aerogel composites were slightly lower than the theoretical values. As shown in Figure 9, the PI/clay aerogel composites exhibited relatively broad decomposition regions ranging from 360 to 670 °C, as a result of the release of residual TEA, the decomposition of the imide ring of PI, and the loss of interlayer water molecules in clay slightly later.

4. CONCLUSIONS

PI/clay aerogel composites were successfully produced from water-soluble polyimide precursor/clay solution, and they had bulk densities of less than 0.1 g/cm^3. The aerogel composites exhibited a layer−strut bracing structure, resulting in an increase in the compressive modulus by as much as 5−50 times compared to that of unmodified clay aerogel. The onset decomposition temperature of the aerogels reached up to 410 °C. The polyimide chain did not intercalate or exfoliate the clay. The improved mechanical performance and excellent heat resistance of the prepared aerogel composites raise the possibility that these modified clay aerogel composites could be used as high-temperature insulation materials.

AUTHOR INFORMATION

Corresponding Author

*E-mail: wangkai@buaa.edu.cn.

Notes

The authors declare no competing financial interest.

REFERENCES

(1) Mackenzie, R. C. Clay−Water Relationships. *Nature* **1953**, *171*, 681−683.
(2) Call, F. Preparation of Dry Clay-Gels by Freeze-Drying. *Nature* **1953**, *172*, 126.
(3) Norrish, K.; Rausell-Colom, J. A. Effect of Freezing on the Swelling of Clay Minerals. *Clay Miner. Bull.* **1962**, *5*, 9−16.
(4) Ahlrichs, J. L.; White, J. L. Freezing and Lyophilizing Alters the Structure of Bentonite Gels. *Science* **1962**, *136*, 1116−1118.
(5) Nakazawa, H.; Yamada, H.; Fujita, T.; Ito, Y. Texture Control of Clay-Aerogel through the Crystallization Process of Ice. *Clay Sci.* **1987**, *6*, 269−276.
(6) Ishikawa, N.; Fujii, K.; Satta, N. The Influence Factor of Structural Change in Kaolinite Suspensions during a Freeze-Drying Process. *Clay Sci.* **2003**, *12*, 167−176.
(7) Leventis, N.; Sotiriou-Leventis, C.; Zhang, G; Rawashdeh, A.-M. M. Nanoengineering Strong Silica Aerogels. *Nano Lett.* **2002**, *2*, 957−960.
(8) Meador, M. A. B.; Fabrizio, E. F.; Ilhan, F.; Dass, A.; Zhang, G.; Vassilaras, P.; Johnston, J. C.; Leventis, N. Cross-Linking Amine-Modified Silica Aerogels with Epoxies: Mechanically Strong Lightweight Porous Materials. *Chem. Mater.* **2005**, *17*, 1085−1098.
(9) Katti, A.; Shimpi, N.; Roy, S.; Lu, H.; Fabrizio, E. F.; Dass, A.; Capadona, L. A.; Leventis, N. Chemical, Physical, and Mechanical Characterization of Isocyanate Cross-Linked Amine-Modified Silica Aerogels. *Chem. Mater.* **2006**, *18*, 285−296.
(10) Meador, M. A. B.; Capadona, L. A.; MacCorkle, L.; Papadopoulos, D. S.; Leventis, N. Structure−Property Relationships in Porous 3D Nanostructures as a Function of Preparation Conditions: Isocyanate Cross-Linked Silica Aerogels. *Chem. Mater.* **2007**, *19*, 2247−2260.
(11) Leventis, N. Three-Dimensional Core-Shell Superstructures: Mechanically Strong Aerogels. *Acc. Chem. Res.* **2007**, *40*, 874−884.

(12) Bandi, S.; Bell, M.; Schiraldi, D. A. Temperature-Responsive Clay Aerogel−Polymer Composites. *Macromolecules* **2005**, *38*, 9216−9220.
(13) Arndt, E. M.; Gawryla, M. D.; Schiraldi, D. A. Elastic Low Density Epoxy/Clay Aerogel Composites. *J. Mater. Chem.* **2007**, *17*, 3525−3529.
(14) Gawryla, M. D.; Nezamzadeh, M.; Schiraldi, D. A. Foam-Like Materials Produced from Abundant Natural Resources. *Green Chem.* **2008**, *10*, 1078−1081.
(15) Pojanavaraphan, T.; Magaraphan, R.; Chiou, B. S.; Schiraldi, D. A. Development of Biodegradable Foamlike Materials Based on Casein and Sodium Montmorillonite Clay. *Biomacromolecules* **2010**, *11*, 2640−2646.
(16) Gawryla, M. D.; Schiraldi, D. A. Novel Absorbent Materials Created via Ice Templating. *Macromol. Mater. Eng.* **2009**, *294*, 570−574.
(17) Alhassan, S. M.; Qutubuddin, S.; Schiraldi, D. Influence of Electrolyte and Polymer Loadings on Mechanical Properties of Clay Aerogels. *Langmuir* **2010**, *26*, 12198−12202.
(18) Alhassan S. M. *Colloidal Interactions and Stability in Processing, Formation and Properties of Inorganic−Organic Nanocomposites*. Ph.D. Thesis, Case Western Reserve University, Cleveland, OH, 2011.
(19) Johnson, J. R., III; Spikowski, J.; Schiraldi, D. A. Mineralization of Clay/Polymer Aerogels: A Bioinspired Approach to Composite Reinforcement. *ACS Appl. Mater. Interfaces* **2009**, *1*, 1305−1309.
(20) Gawryla, M. D.; Liu, L.; Grunlan, J. C.; Schiraldi, D. A. pH Tailoring Electrical and Mechanical Behavior of Polymer−Clay−Nanotube Aerogels. *Macromol. Rapid Commun.* **2009**, *30*, 1669−1673.
(21) Finlay, K.; Gawryla, M. D.; Schiraldi, D. A. Biologically Based Fiber-Reinforced/Clay Aerogel Composites. *Ind. Eng. Chem. Res.* **2008**, *47*, 615−619.
(22) Gawryla, M. D.; van den Berg, O.; Weder, C.; Schiraldi, D. A. Clay Aerogel/Cellulose Whisker Nanocomposites: A Nanoscale Wattle and Daub. *J. Mater. Chem.* **2009**, *19*, 2118−2124.
(23) Meador, M. A. Recent Advances in the Development of Processable High-Temperature Polymers. *Annu. Rev. Mater. Sci.* **1998**, *28*, 599−630.
(24) Hergenrother, P. M. The Use, Design, Synthesis, and Properties of High Performance/High Temperature Polymers: An Overview. *High Perform. Polym.* **2003**, *15*, 3−45.
(25) Kawagishi, K.; Saito, H.; Furukawa, H.; Horie, K. Superior Nanoporous Polyimides via Supercritical CO_2 Drying of Jungle-Gym-Type Polyimide Gels. *Macromol. Rapid Commun.* **2007**, *28*, 96−100.
(26) Chidambareswarapattar, C.; Larimore, Z.; Sotiriou-Leventis, C.; Mang, J. T.; Leventis, N. One-Step Room-Temperature Synthesis of Fibrous Polyimide Aerogels from Anhydrides and Isocyanates and Conversion to Isomorphic Carbons. *J. Mater. Chem.* **2010**, *20*, 9666−9678.
(27) Leventis, N.; Sotiriou-Leventis, C.; Mohite, D. P.; Larimore, Z. J.; Mang, J. T.; Churu, G.; Lu, H. Polyimide Aerogels by Ring-Opening Metathesis Polymerization (ROMP). *Chem. Mater.* **2011**, *23*, 2250−2261.
(28) Guo, H.; Meador, M. A. B.; McCorkle, L.; Quade, D. J.; Guo, J.; Hamilton, B.; Cakmak, M.; Sprowl, G. Polyimide Aerogels Cross-Linked through Amine Functionalized Polyoligomeric Silsesquioxane. *ACS Appl. Mater. Interfaces* **2011**, *3*, 546−552.
(29) Meador, M. A. B.; Malow, E. J.; Silva, R.; Wright, S.; Quade, D.; Vivod, S. L.; Guo, H.; Guo, J.; Cakmak, M. Mechanically Strong, Flexible Polyimide Aerogels Cross-Linked with Aromatic Triamine. *ACS Appl. Mater. Interfaces* **2012**, *4*, 536−544.
(30) Somlai, L. S.; Bandi, S. A.; Schiraldi, D. A. Facile Processing of Clays into Organically-Modified Aerogels. *AIChE J.* **2006**, *52*, 1162−1168.
(31) Nayak, P. S.; Singh, B. K. Instrumental Characterization of Clay by XRF, XRD and FTIR. *Bull. Mater. Sci.* **2007**, *30*, 235−238.
(32) Kim, S. K.; Kwen, H. D.; Choi, S. H. Radiation-Induced Synthesis of Vinyl Copolymer Based Nanocomposites Filled with Reactive Organic Montmorillonite Clay. *Radiat. Phys. Chem.* **2012**, *81*, 519−523.
(33) Pojanavaraphan, T.; Magaraphan, R. Prevulcanized Natural Rubber Latex/Clay Aerogel Nanocomposites. *Eur. Polym. J.* **2008**, *44*, 1968−1977.
(34) Pojanavaraphan, T.; Schiraldi, D. A.; Magaraphan, R. Mechanical, Rheological, and Swelling Behavior of Natural Rubber/Montmorillonite Aerogels Prepared by Freeze-Drying. *Appl. Clay Sci.* **2010**, *50*, 271−279.
(35) Kinney, J. H.; Marshall, G. W.; Marshall, S. J.; Haupt, D. L. Three-Dimensional Imaging of Large Compressive Deformations in Elastomeric Foams. *J. Appl. Polym. Sci.* **2001**, *80*, 1746−1755.
(36) Podsiadlo, P.; Kaushik, A. K.; Arruda, E. M.; Waas, A. M.; Shim, B. S.; Xu, J.; Nandivada, H.; Pumplin, B. G.; Lahann, J.; Ramamoorthy, A.; Kotov, N. A. Ultrastrong and Stiff Layered Polymer Nanocomposites. *Science* **2007**, *318*, 80−83.